

GaN Quantum Dots: Physics and Applications

Le Si DANG,* G. FISHMAN and H. MARIETTE

*Laboratoire Spectrometrie Physique (CNRS UMR 5588),
Universite J. Fourier-Grenoble, BP 87, F-38402 Saint Martin d'Herès Cedex, France*

C. ADELMANN, E. MARTINEZ, J. SIMON, B. DAUDIN, E. MONROY, N. PELEKANOS and J. L. ROUVIERE
CEA/DRFMC/SP2M, 17 rue des Martyrs, F-38054 Grenoble Cedex 9, France

Y. H. CHO

Department of Physics, Chungbuk National University, Cheongju 361-763

Recent works by our group on hexagonal and cubic GaN/AlN quantum dots grown by molecular beam epitaxy are reviewed. It is shown that the growth of GaN on AlN can occur either in a layer-by-layer mode to form quantum wells or in the Stranski-Krastanow mode to form self-assembled quantum dots. High resolution transmission electron microscopy reveals that quantum dots are truncated pyramids (typically 3 nm high and 15 nm wide), nucleating on top of a wetting layer. The existence of internal electric fields of 7 MV/cm in hexagonal quantum dots is evidenced by observations of various physical effects related to the quantum confined Stark effect, *e.g.* energy redshift of the interband transition, decrease of its oscillator strength, or enhancement of the exciton interaction with LO phonons. Prospects for UV and near-IR applications, using interband and intersubband transitions of GaN/AlN quantum dots, respectively, will be discussed also in this presentation.

PACS numbers: 68.65.Hb, 73.63.Kv, 78.55.Cr, 78.67.Hc, S7.14

Keywords: Self-assembled quantum dot, Nitride semiconductors, Excitons, Quantum confined Stark effect

I. INTRODUCTION

In semiconductor physics, quantum dots (QDs) are the ultimate three-dimensional (3D) confinement structures of carriers. They can be considered as artificial atoms, with discrete energy levels and reduced density of states (DOS). Their unusual electronic properties, mostly due to the nanometer scale of the confinement potential, have attracted increasing interests and a recent review of their physical studies and device applications can be found in ref[1]. In this paper, we present a brief summary of GaN/AlN QDs which are much less well known than their II-VI (CdTe/ZnTe, CdSe/ZnSe) or III-V (InAs/GaAs) counterparts. It will be shown, in Section II, that nitride QDs are a model system to investigate the various energetic and kinetic processes governing the growth of QDs by molecular beam epitaxy (MBE). In Sections III and IV, we discuss some new physical situations and device applications deriving from the unique properties of nitride semiconductors. Finally in section V, the main conclusions are summarized.

II. MBE OF GaN/AlN QDS

The lattice mismatch between GaN and AlN is about 2.4 %. Recently it has been shown that two distinct procedures [2] can be used to grow GaN/AlN QDs in the wurtzite (hexagonal) crystalline phase by MBE (substrate 6H-SiC and growth temperature ~ 700 °C). The first one, requiring the deposition of GaN on AlN under N-rich conditions, is the well known Stranski-Krastanow (SK) growth mode in which elastic energy stored in the two-dimensional (2D) GaN layer is released by the spontaneous formation of 3D islands. As shown in Fig. 1, the 2D to 3D transition occurs after 3 monolayers (MLs) of GaN have been deposited. For the second growth procedure, GaN is grown on AlN under Ga-rich conditions, in the presence of a self-regulated Ga film (about 2 MLs) on top of the 2D GaN layer. The Ga bilayer completely modifies the surface energy of the heteroepitaxial layer, and maintains its 2D character well beyond the SK critical thickness (see Fig. 1). It should be noted that there is no change on the in-plane lattice parameter of the heterostructure, and thus no misfit dislocation network would be introduced at this stage, even for 6 deposited GaN MLs. This 2D metastability is destroyed, however, by a growth interruption and a new equilibrium state is

*E-mail: lesidang@spectro.ujf-grenoble.fr

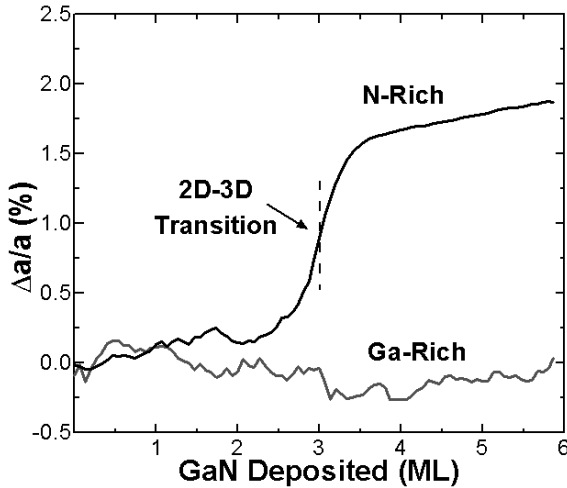


Fig. 1. Variations of the in-plane lattice mismatch of the epitaxial layer as a function of the number of GaN MLs deposited on AlN, for two growth conditions : N-rich and Ga-rich. In the former case, the 2D to 3D transition (SK mode) occurs after 3 MLs of GaN have been deposited. In the latter case, the epitaxial layer remains 2D for thickness well beyond the SK critical thickness, without any generation of misfit dislocation network.

reached with the spontaneous generation of QDs. More details on MBE of these nitride QDs are given in ref[2].

Fig. 2 is an image of a multi-layer QD structure obtained by high resolution transmission electron microscopy [3]. GaN/AlN QDs appear as truncated pyramids, with an average height of 3 nm, and a base about 5 times larger, nucleating on top of a wetting layer. A clear vertical correlation can be observed for typical interlayer distance of about 10 nm. Average densities of SK QDs are in the $10^{11}/\text{cm}^2$ range, whereas one can vary the densities of the second type of QDs between $10^{10}/\text{cm}^2$ and $10^{11}/\text{cm}^2$ by changing the thickness of the GaN layer before growth interruption. GaN/AlN QDs in the zinc blende (cubic) phase can also be obtained by MBE via the SK mode [4]. Their structural characteristics (size, density) are similar to those of hexagonal QDs.

III. OPTICAL PROPERTIES

Fig. 3 shows the low temperature photoluminescence (PL) spectra of two samples of hexagonal GaN/AlN QDs of large sizes (“with ripening” in the figure, height of 4.1 nm as determined by high resolution transmission electron microscopy) and small sizes (“without ripening”, 2.3 nm). Their peak energies are below and above the GaN bandgap energy, respectively, differing by as much as 0.8 eV. By contrast, PL spectra of cubic QDs (not shown) are systematically observed at higher energies than the GaN bandgap energy.

The origin of this remarkable spectral variation of

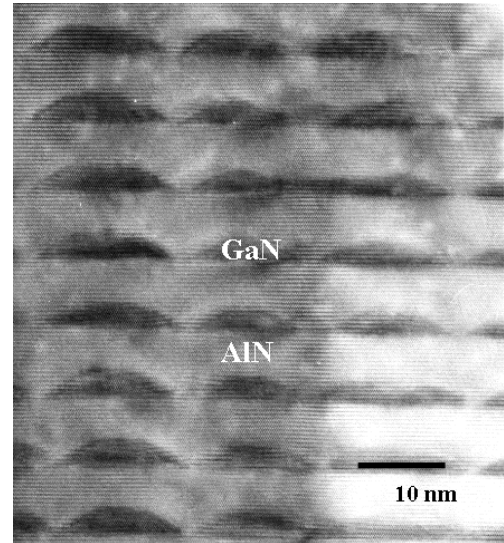


Fig. 2. Image by high resolution transmission electron microscopy of a multi-layers of hexagonal GaN/AlN QDs. Vertical correlation of QD nucleation is observed for interlayer distance of about 10 nm.

hexagonal QD interband transitions is the quantum confined Stark effect, due to the presence of a giant internal electric field $|F| \approx 7 \text{ MV/cm}$ induced by the spontaneous and piezoelectric polarizations along the QD height (also crystal *c*-axis) [5]. The interband transition energy is well described by :

$$E(d) \approx E_g + E_e + E_h - Fd, \tag{1}$$

where E_g is the bandgap energy of GaN, $E_{e(h)}$ is the electron (hole) confinement energy, and d is the QD height. In practice, E_e and E_h do not vary much with the QD size for $d \geq 2 \text{ nm}$, since electrons and holes are repelled by the strong electric field at opposite interfaces, and confined in a (similar) triangular profile potential.

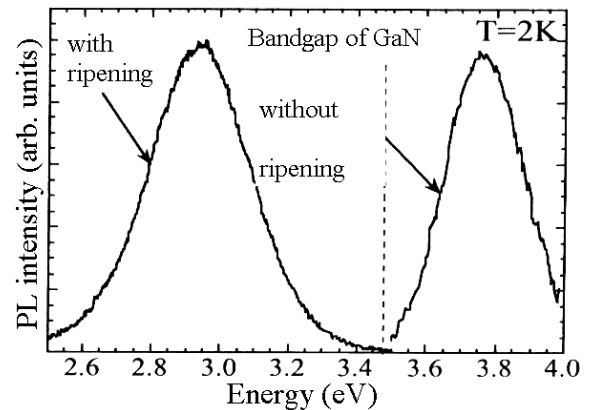


Fig. 3. Low temperature PL of hexagonal GaN/AlN QDs of different heights : 4.1 nm (with ripening) and 2.3 nm (without ripening). The bandgap energy of bulk GaN is marked by the dotted line.

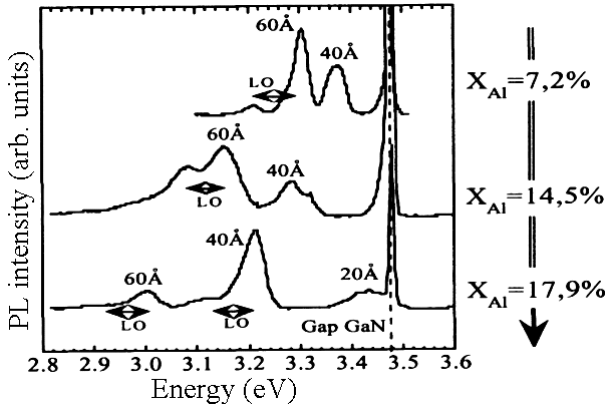


Fig. 4. Low temperature PL of hexagonal GaN/AlGaN QWs of different QW widths and Al barrier contents. The internal electric field increases with increasing Al contents (from top to bottom of figure). Note that the strongest LO phonon replica of the 60 Å QW is observed for the intermediate electric field (see text).

The spatial separation of electrons and holes by the internal electric field in hexagonal QDs should strongly modify their other electronic properties as well. For example, the Fröhlich coupling to LO phonons is expected to be enhanced since electrons and holes are spatially distributed as for an electric dipole. On the other hand, the reduced e-h Coulomb interaction tends to increase the in-plane exciton Bohr radius, so that the Fröhlich coupling should vanish for very large QDs and/or very large electric field. Some evidence of these two opposite effects could be observed in Fig. 4, which displays the PL spectra of GaN/AlGaN quantum wells (QWs) of different well widths and barrier Al contents. In the figure, the 40 and 60 Å QWs clearly shift to the red with increasing Al contents, which can be accounted for by an increasing internal electric field. However it can be seen that the LO phonon replica of the 60 Å QW is the strongest for the intermediate electric field. This indicates that the “Bohr radius” negative effect on the Fröhlich coupling is dominant over the “electric dipole” positive effect in the case of the strongest electric field.

Fig. 5. shows a comparative study of the low temperature radiative decay time of hexagonal and cubic QDs. The marked increase of hexagonal QD decay time with increasing height is well reproduced by a model calculation assuming the existence of an internal electric field of 7 MV/cm, in very good agreement with ref[5]. For cubic QDs, the decay time is shorter by one order of magnitude in average, and only weakly dependent on the QD size since there is no quantum confined Stark effect as for hexagonal QDs. At first thought, one may conclude that hexagonal QDs could be extremely sensitive to non-radiative processes, for at least two reasons : i), the radiative decay times are very long, in the scale of 10 ns in average ; ii), electron and hole wavefunctions extend more into the barrier material, even for large QDs,

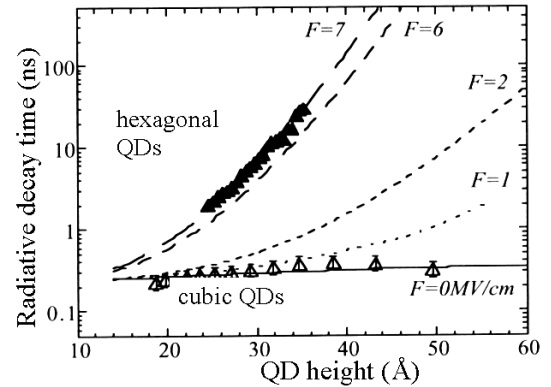


Fig. 5. Low temperature radiative decay time of hexagonal and cubic GaN/AlN QDs as a function of dot height. Dotted and solid curves are model calculations.

as a result of the strong internal electric field. In fact, PL data in Fig. 6 clearly show that the radiative quantum efficiency of hexagonal QDs is remarkably high at room temperature : the PL intensity of resonantly excited QDs decreases by less than 50 % as compared to the low temperature measurements. This exceptional behavior could be due to two factors : first, the QD density (in the $10^{11}/\text{cm}^2$ range) is much higher than for defects; second, carriers in GaN are efficiently confined and thermally stable due to the record difference in bandgap energies between GaN (3.6 eV) and AlN (6.2 eV).

Fig. 6 shows also that carriers in QWs are more subject to non-radiative defects, as a result of their 2D degree of freedom. Another convincing illustration of the superiority of QD as an efficient radiative recombination center is displayed in Fig. 7. In the figure, we report a cathodoluminescence study at $T = 80\text{K}$ of a separate confinement heterostructure laser sample consisting of QD multi-layers inserted in a AlGaIn/AlN optical waveguide. The cathodoluminescence images of the AlGaIn 2D barrier (emitting at 308 nm) and GaN QD (emitting at

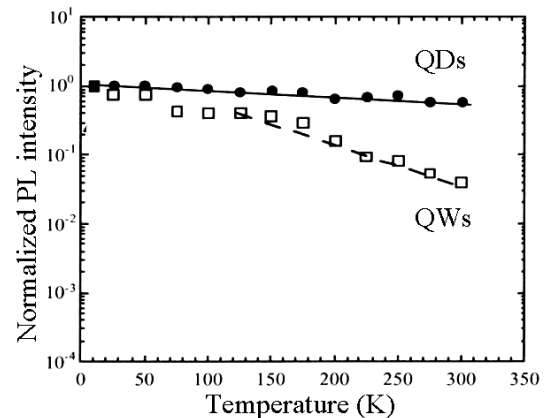


Fig. 6. Temperature dependence of PL of hexagonal GaN/AlN QD and QW under resonant excitation (below AlN barrier).

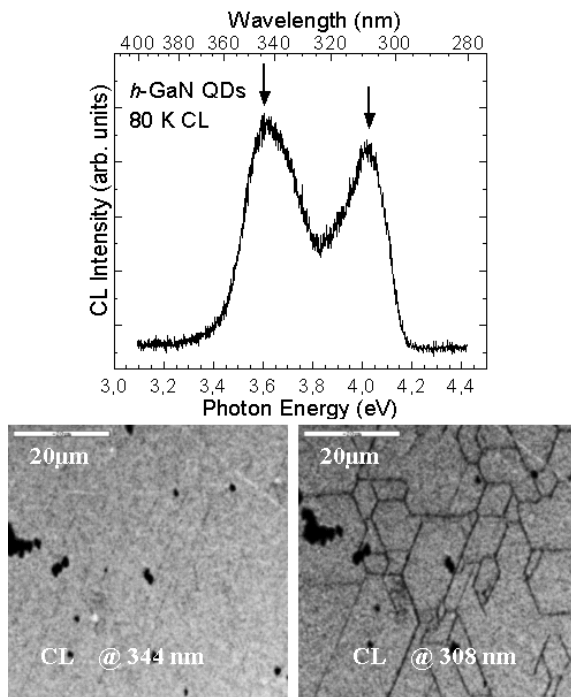


Fig. 7. Cathodoluminescence spectrum of a separate confinement heterostructure consisting of GaN QD multi-layers inserted in a AlGaN/AlN optical waveguide ($T = 80$ K). Bottom : Cathodoluminescence images at 308 nm (AlGaN barrier) and at 344 nm (GaN QD).

344 nm) differ by the presence of dark line defects (probably joint defects) in the former. These defects exist in the whole heterostructure, but only carriers trapped in QDs are not affected.

IV. DEVICE APPLICATIONS

GaN/AlN QDs are attractive for device applications since they combine many unique features of QDs and wide bandgap materials. We will discuss two promising optoelectronic applications in the UV and near-IR spectral domains.

1. UV laser

Nitride semiconductors are well suited for UV lasers based on interband transitions. Their effective masses are, however, much heavier than those of smaller bandgap semiconductors such as GaAs. Therefore conventional nitride QW lasers would require much higher thresholds because of their higher 2D DOS. In this respect, a GaN/AlN QD laser, with discrete energy levels and reduced 0D DOS, is a good candidate for a low

threshold UV laser [6]. Another major advantage of using QDs instead of QWs is the benefit of carrier localization when considering the lack of high quality substrates currently available for epitaxial growth.

2. IR unipolar optoelectronics

Intersubband transition is unipolar since it involves only one type of carrier (electron or hole) making transition between two of its levels within the same (conduction or valence) band. By contrast to other semiconductors such as GaAs/AlGaAs, the huge bandgap energy difference in nitride semiconductors (2.6 eV between GaN and AlN) should allow record tuning of electron intersubband transitions to cover the near-IR region (1.5-4.0 μm) of interests for telecommunication applications based on optical fibers. Indeed strong intersubband absorptions in the spectral range between 1.4 and 4.2 μm have been reported recently in GaN/AlGaN multi-QWs [7]. However, two factors could favor QDs for practical applications : i), normal incidence is forbidden for electron intersubband transitions in QWs (dipole aligned along the confinement axis) but not in QDs; ii), the electron scattering time between subbands in nitride QWs is found to be in the sub-picosecond range [7], which is attractive for high-speed photodetector applications, but could be a limiting factor for laser applications. To our knowledge, the electron scattering time has not been measured in nitride QDs yet, but could be significantly longer due to the discrete energy level structure.

V. CONCLUSIONS

In this short review, we show that the growth of GaN on AlN by MBE can occur either in a layer-by-layer mode to form QWs or in the Stranski-Krastanow mode to form self-assembled QDs. High resolution transmission electron microscopy reveals that QDs are truncated pyramids. The existence of internal electric fields of 7 MV/cm in hexagonal QDs is evidenced by the observation of various physical effects related to the quantum confined Stark effect, *e.g.* redshift of the interband transition energy, decrease of its oscillator strength, or enhancement of the exciton interaction with LO phonons. Prospective developments of a UV low threshold laser and near-IR applications in the optical fiber domain (1.5-4.2 μm) are attractive, using interband and intersubband transitions of GaN/AlN QDs, respectively.

ACKNOWLEDGMENTS

The authors was done in the Nanophysics and Semiconductors group of the CEA-CNRS-UJF. The would

would like to acknowledge the contribution of Dr. H. M. Kim for the cathodoluminescence experiments. Y. H. Cho was supported by KOSEF through QSRC at Dongguk University in 2002.

REFERENCES

- [1] *Proceedings of the International Conference on Semiconductor Quantum Dots (QD 2000)* (Munich, Germany, 2000), edited by U. Woggon and A. Zrenner, Phys. Stat. Sol. (b) **224**, Number 1-3 (Wiley-VCH).
- [2] C. Adelman, J. Brault, J.-L. Rouviere, H. Mariette, Guido Mula and B. Daudin, J. Appl. Phys. **91**, 5498 (2002); C. Adelman, J. Brault, D. Jalabert, P. Gentile, H. Mariette, Guido Mula and B. Daudin, J. Appl. Phys. **91**, 9638 (2002); *Int. Workshop on Nitride Semiconductors* (Aachen, Germany, 2002).
- [3] M. Arlery, J. L. Rouviere, F. Widmann, B. Daudin, G. Feuillet and H. Mariette, Appl. Phys. Lett. **74**, 3287 (1999).
- [4] E. Martinez-Guerrero, C. Adelman, F. Chabuel, J. Simon, N. T. Pelekanos, Guido Mula, B. Daudin, G. Feuillet and H. Mariette, Appl. Phys. Lett. **77**, 809 (2000).
- [5] F. Widmann, J. Simon, B. Daudin, G. Feuillet, J. L. Rouviere, and N. T. Pelekanos and G. Fishman, Phys. Rev. B **58**, R15989 (1998).
- [6] Y. Arakawa, T. Someya and K. Tachibana, Phys. Stat. Sol. (b) **224**, 1 (2001).
- [7] H.M. Ng, C. Gmachl, T. Siegrist, S. Chu and A. Cho, Phys. Stat. Sol. (a) **188**, 825 (2001); N. Iizuka, K. Kaneko, N. Suzuki, T. Asano, S. Noda and O. Wada, Appl. Phys. Lett. **77**, 648 (2000).